



Effect of silicon source on the crystallization temperature of the cordierite

Hajjou Hanaa¹, Saâdi Latifa^{1*}, Waqif Mohamed¹, Fatah Nouria²

¹Laboratoire de Matière Condensée et Nanostructures (LMCN), Faculté des Sciences et Techniques Guéliz, Université Cadi Ayyad, BP 549, Marrakech, Morocco.

²Ecole Nationale Supérieure de Chimie de Lille, Cité scientifique 59650, Ville neuve d'Ascq, Unité de Catalyse et de Chimie du Solide, UMR 8181 CNRS, Université Lille1.

Received 20 Nov 2014, Revised 07 Oct 2015, Accepted 10 Oct 2015

*Corresponding author: Email: la.saadi@yahoo.fr; Tel: +212611747591

Abstract

The effect of different silicon sources - silica gel SiO₂, tetraethylorthosilicate Si (OC₂H₅)₄ and silicic acid H₂Si₂O₅ - on the crystallization of cordierite were investigated. Aluminum chloride (AlCl₃·6H₂O) and magnesium chloride (MgCl₂·6H₂O) were respectively used as sources of Aluminum and magnesium. The precursors of cordierite were prepared through the coprecipitation method. The different starting materials were mixed in an aqueous medium in stoichiometric proportions of the cordierite (2Al₂O₃, 2MgO, 5SiO₂). Different experimental techniques (TGA, X-ray, IR, SEM and dilatometry) were used to characterize the prepared precursors. The obtained results indicated the presence of several crystalline phases such as mullite, spinel, corundum, enstatite, cristobalite at low temperature (1000 °C, 1100 °C) beside the amorphous phase. At 1200 °C, the crystallization of μ-cordierite was observed; this crystalline phase was transformed into α-cordierite (Indialite) at 1300 °C. By increasing the temperature up to 1400 °C the main phase obtained is α-cordierite with an amount of spinel that varies with the silicon sources. The morphological analysis showed that the shape and the size of grains of α-cordierite phase were influenced by the nature of silicon source.

Keywords: cordierite, silicon, calcination, spinel, coprecipitation.

1. Introduction

Cordierite (2MgO·2Al₂O₃·5SiO₂) is one of magnesium aluminosilicate materials that exhibit excellent physical properties [1-4] such as excellent thermal resistance, high refractivity, high mechanical strength and high durability. Therefore, it's widely used as micro-filtration membranes, as honeycomb-shaped catalyst carriers in automobile exhaust systems, as substrate material for integrated circuit boards and as refractory materials [5-10].

Several synthesis methods of cordierite have been studied in the literature, mostly solid state reaction and coprecipitation. In most previous studies, cordierite was prepared from a mixture of natural products (kaolin, talc, quartz and giobertite ...) or synthetic products, calcined at high temperature [10-21].

Goren et al. [10] had synthesized the cordierite from raw material mixture containing talc, diatomite and alumina. Furthermore, the same authors had synthesized the cordierite using a composition prepared by the mixture of talc, fly ash, fused silica and alumina [11]. In both studies, the α-cordierite was obtained at 1300 °C as an important phase along with spinel and cristobalite as secondary phase.

As well, Aklouche [12] has prepared the cordierite precursors by solid state reaction using kaolin and magnesium hydroxide (Mg (OH)₂) in the stoichiometric proportions. The evolution of the infrared spectra and X-ray diffraction patterns showed that the crystallization of α-cordierite take place in the range of [1300 °C-1400 °C].

Benito et al. [13] synthesized cordierite precursors from a mixture of talc, kaolin and hydromagnesite (Mg₄(CO₃)₃(OH)₂·3H₂O). The presence of μ-cordierite and spinel phase was noted from 1150°C. While increasing the temperature up to 1300 °C, the crystallization of α-cordierite was observed along with the formation of mullite, cristobalite and spinel as a secondary phase.

During the last few years, cordierite was mainly obtained using sol-gel method [1, 14, 15], which offers many assets to produce materials with greater homogeneity and purity.

The sol-gel preparation method was used by Menchi et al. [14] to prepare the cordierite. The aluminum acetate gel, tetraethylorthosilicate (TEOS), magnesium acetate solution, ethanol and phenol-formaldehyde resin have been used. The formation of α -cordierite is visible at 1246 °C, with the cristobalite, sapphirine and magnesium-aluminum silicate.

Naskar et al. [15] have synthesized the cordierite by sol-gel technique using two different silica sources TEOS and fumed silica beside the rice hush ash, an agro-based waste material. The α -cordierite was found to be formed in the temperature range of [1320 – 1365 °C]. It is noted that the formation of intermediate phases depends on the starting used materials.

Demand for cordierite is increasing more and more, therefore it is necessary to improve the conditions of its synthesis. Several studies have been conducted in this regard, however, many related constraints were still present, a very high crystallization temperature, presence of secondary phases, as well as problems accrued during sintering.

The previous works revealed that the synthesis of cordierite depends on several parameters (type of reagents, composition, sintering temperature ...), these factors have a certain influence on the physicochemical properties of the obtained solid, hence in this study, the effect of silicon source on the crystallization behavior of cordierite has been elucidated. The structural and phases transformation were investigated for different temperatures of calcinations using several analysis techniques.

2. Experimental procedure

2.1. Preparation of precursors

The precursors were prepared from a mixture of metal salts, aluminum chloride, magnesium chloride and different sources of silicon; silica gel, silicic acid and TEOS; the samples were respectively referenced as AMGS, AMAS and AMES according to the silicon source. The silicic acid was obtained by an exchange with a cationic resin according to the protocol used by Saadi et al [22] for the preparation of mullite precursors.

The precursors were prepared by mixing the starting reactants in the stoichiometric proportions of cordierite ($2\text{MgO} \cdot 2\text{Al}_2\text{O}_3 \cdot 5\text{SiO}_2$) in an aqueous medium. The mixture was heated under reflux for 4 h. After filtration the powder was dried in the oven for 24h at 110 °C, the obtained powders were pre-calcined at 600 °C for 2 hours, followed by calcination at temperatures between 1000 °C and 1400 °C in a muffle furnace with a heating rate of 5 °C/min. The prepared precursors were analyzed in raw and calcined state.

2.2 Experimental techniques

The physicochemical characterization of the prepared precursors was carried out using several experimental techniques. The thermogravimetric analysis was performed using a thermal apparatus type Versa Therm, under nitrogen atmosphere, with a heating rate of 10 °C/min. The X-ray diffraction analysis was carried out using a Philips diffractometer type PW X'Pert MPD with a copper anticathode ($\lambda_{\text{K}\alpha}=1.5406\text{\AA}$). The identification of the present phases was determined using the software highscore. The Infrared spectroscopic analysis was performed using a Perkin Elmer Spectrometer, in wavenumber range [4000 - 400 cm^{-1}] with 4 cm^{-1} resolution. A dilution of the sample to 2% was achieved in KBr. The assignment of the different absorption bands was made through the data set in the literature [12-15]. The dilatometric tests were carried out using a Setaram apparatus, at a heating rate of 1 °C/min from room temperature to 1400 °C. The Microscopic observations were performed on the samples calcined at 1400 °C, using a scanning electron microscope types Jeol JSM 5500. The samples were first metalized by vacuum deposition of carbon.

3. Results and discussion

3.1. Characterization of raw precursors

3.1.1. Thermo-gravimetric analysis

The TGA curves of the three precursors, Figure 1, have the same tendency. The rate of weight loss is a little different from a precursor to another; it exceeds 50% by weight of the raw sample. The weight loss occurs so rapidly since 200 °C. The maximum weight loss is observed between 100 °C and 400 °C. Therefore, a pretreatment at 400 °C is necessary to remove excess water and all the volatile elements that exist in the different precursors elaborated [11].

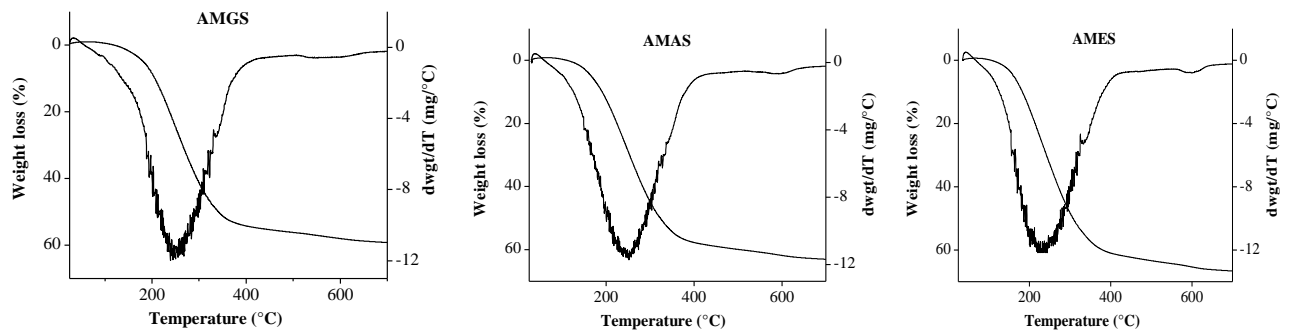


Figure 1: Gravimetric Analysis of samples AMGS, AMAS and AMES.

3.1.2. Mineralogical analyzes (XRD, IR)

a) Analysis by X-ray diffraction

Figure 2 shows the X-ray diffraction patterns of all precursors in the raw state. An intense and sharp peaks corresponding to the magnesium aluminate ($MgAl_2O_4$) has been observed for the sample AMAS along with some weaker peaks corresponding to Periclase (MgO). Furthermore, the sample AMGS diffractogram shows some peaks corresponds to hydrated magnesium oxychloride ($Mg_2(OH)_3Cl \cdot 4(H_2O)$). While in the case of the AMES precursor, the presence of aluminum chloride ($AlCl_3$) and hydrated magnesium chloride ($MgCl_2 \cdot 6H_2O$) is evidenced. Therefore, this difference in the XRD patterns proves that the silicon source affects the mineralogical composition of precursors prepared in an aqueous medium.

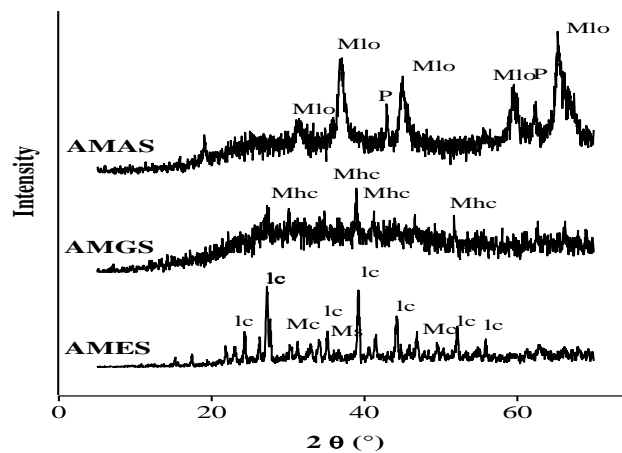


Figure 2: XRD patterns of the AMES, AMGS and AMAS samples in the raw state. (Mhc: magnesium chloride hydroxide, lc: aluminum chloride, Mc: hydrated magnesium chloride, Ms: magnesium silicate, Mlo: magnesium aluminum oxide, P: periclase).

b) Analysis by infrared spectroscopy (IR):

The samples AMES and AMGS have similar spectra but different from that of AMAS (Fig. 3). In fact, the three precursors exhibit similar bands of absorption in the wavenumber range $4000 - 1500 \text{ cm}^{-1}$. The presence of broad band in the wavenumber range $3600 - 3000 \text{ cm}^{-1}$ can be easily associated to characteristic absorption band of OH groups in hydroxyl phases [22], while the absorption band at around 1600 cm^{-1} , is associated to the vibration of OH groups in H_2O . However the spectra in the wavenumber range $1500 - 400 \text{ cm}^{-1}$ revealed:

- for the AMES and AMGS samples the presence of a band at around 600 cm^{-1} due to the condensed AlO_6 octahedra [15]
- for the AMAS sample the presence of a characteristic shoulder in the region $1100 - 1100 \text{ cm}^{-1}$ assigned to the Si-O-Si asymmetric stretching vibration [11], around 700 cm^{-1} a characteristic band of the spinel

(MgAl_2O_4) and a band at around 550 cm^{-1} characteristic of the Al-O stretching vibration in isolated AlO_6 octahedra [15].

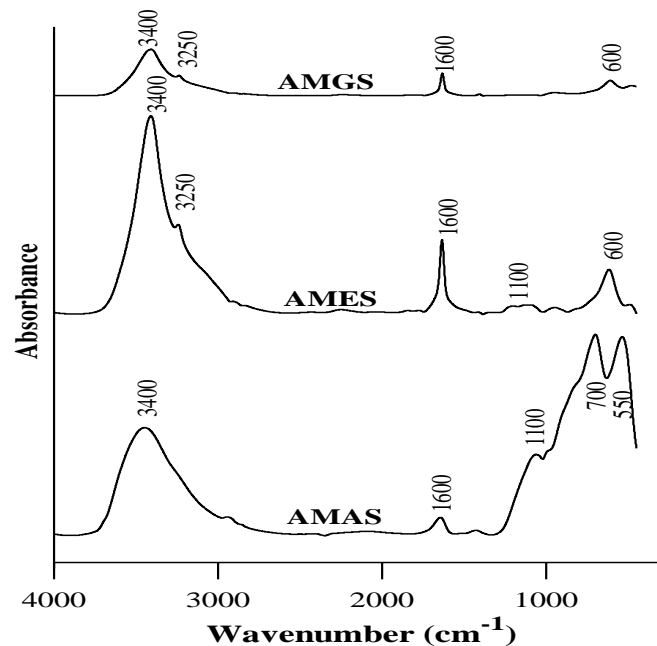


Figure 3: Infrared spectra of the AMAS, AMES and AMGS samples in the raw state.

3.2. Analysis of the calcined samples

3.2.1. Mineralogical analysis (XRD, IR)

The evolution of the mineralogical composition (XRD and IR), depending on the calcination temperature (1000 to $1400\text{ }^\circ\text{C}$) of the different samples studied, is shown in fig. (4 - 9).

- **AMES sample**

The diffraction pattern of the AMES sample calcined at $1000\text{ }^\circ\text{C}$ shows the existence of characteristic peaks of the mullite phase ($3\text{Al}_2\text{O}_3 \cdot 2\text{SiO}_2$) (3.39 , 3.42 and 2.54 \AA) (Fig. 4). Moreover, the presence of this phase is confirmed by shoulders in the IR spectrum at 1175 , 950 and 897 cm^{-1} (Fig. 5) [23]. It is noteworthy that, at this temperature the peaks at 2.43 , 1.55 and 1.42 \AA can be attributed to the spinel phase MgAl_2O_4 . This is also confirmed by the appearance of characteristic bands of spinel at 560 , 700 and 800 cm^{-1} [8]. The spinel phase is a result of interaction between $[\text{AlO}_6]$ and $[\text{MgO}_6]$ [11, 15].

At $1100\text{ }^\circ\text{C}$, the formation of enstatite ($\text{Mg}_2\text{Si}_2\text{O}_6$) (3.15 , 3.17 and 2.78 \AA), and also an increase in the intensity of the diffraction peaks of the spinel phase 2.43 ; 2.02 and 1.42 \AA has been observed. The further rise in temperature to $1200\text{ }^\circ\text{C}$, causes the crystallization of free silica cristobalite (4.04 , 2.84 and 2.48 \AA) and the formation of corundum (2.08 , 2.55 and 1.60 \AA) [11]. Also at this temperature a partial reaction of the spinel phase with amorphous silica to form the μ -cordierite was observed [14, 15, 24]. This is confirmed by the decrease in the intensity of the characteristic peaks of the spinel phase and the appearance of new bands at 1085 , 935 and 700 cm^{-1} assigned to the μ -cordierite (Fig. 5) [15].

At $1300\text{ }^\circ\text{C}$, the appearance of the characteristics peaks of the α -cordierite phase at 8.48 , 3.13 and 3.02 \AA was noted. This was again confirmed by the IR spectra with the appearance of characteristic bands at 1185 , 1140 , 950 and 770 cm^{-1} [15].

At $1400\text{ }^\circ\text{C}$ the spectrum shows the α -cordierite phase as the main phase accompanied by the spinel as a secondary phase. Thus the result of mineralogical analysis by X-ray diffraction and IR spectroscopy shows that the precursor AMES undergoes a succession of phase transformations with temperature. In fact at low temperature ($1000\text{ }^\circ\text{C}$), we observed the formation of spinel and mullite. Furthermore, the crystallization of cristobalite, corundum and μ -cordierite occurred at temperatures between $1100\text{ }^\circ\text{C}$ and $1200\text{ }^\circ\text{C}$. At $1300\text{ }^\circ\text{C}$, we had the formation of α -cordierite. At $1400\text{ }^\circ\text{C}$ α -cordierite was obtained as the main phase accompanied by the spinel phase as a secondary phase.

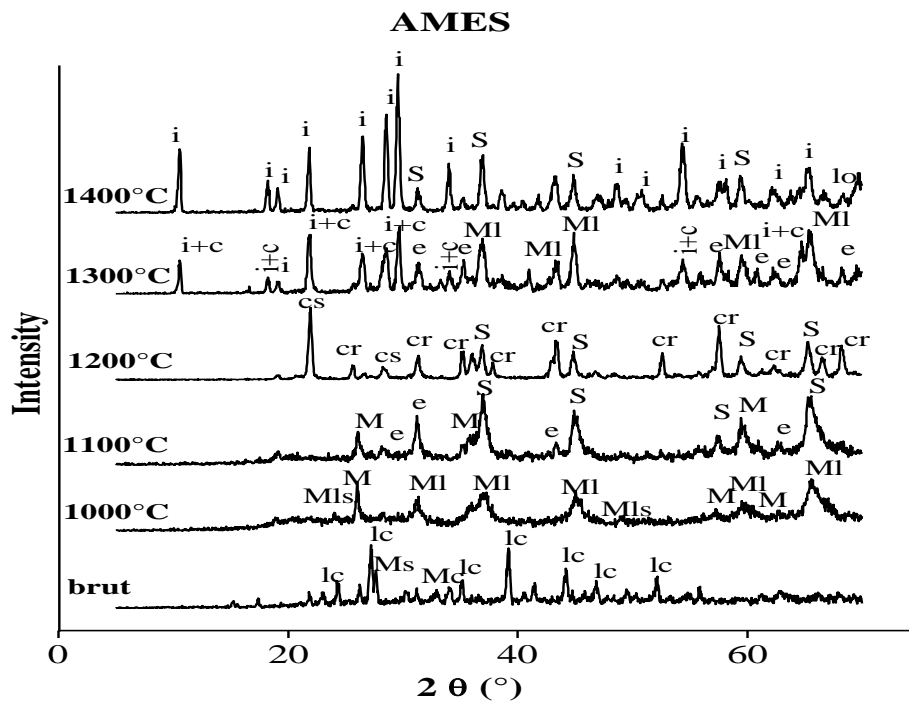


Figure 4 : XRD patterns of the AMES samples raw and calcined at various temperatures. (Ms: magnesium silicate, MI: magnesium aluminum oxide, Mls: magnesium aluminum silicate, M: mullite, cs: cristobalite, cr: corundum, c: μ -cordierite, i: indialite, S: Spinel, Mo: oxide magnesium, e: Enstatite)

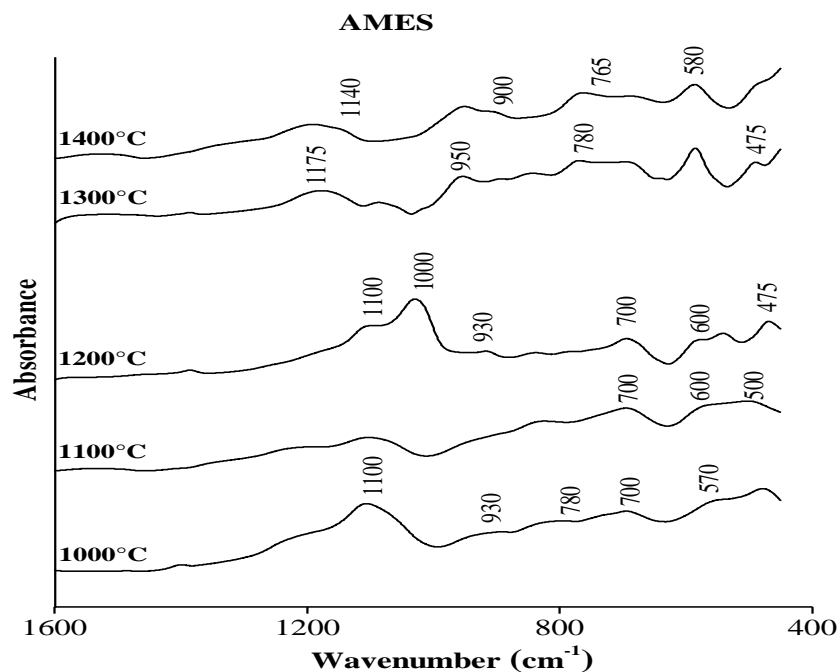


Figure 5: Infrared spectra of the AMES sample calcined at different temperature.

• **AMGS sample :**

The XRD spectra of the AMGS sample calcined at 1000 °C shows the presence of characteristic peaks of magnesium oxide (MgO) (2.43, 2.11 and 1.49 Å), aluminum oxide (Al₂O₃) (2.39, 1.98 and 1.39 Å), enstatite (3.15, 3.17 and 2.78 Å), and spinel (MgAl₂O₄) (Fig. 6). This is reflected in the IR spectrum by the appearance of characteristic bands of the spinel phase at 560, 700 and 800 cm⁻¹. Crystallization of the spinel is due to the reaction between aluminum and the MgO formed by the dissociation of magnesium chloride [10, 15].

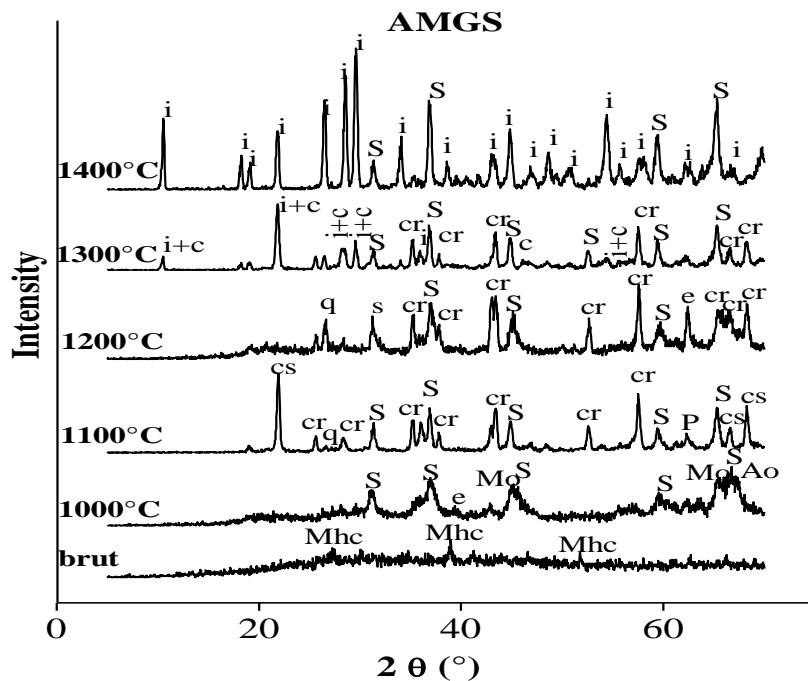


Figure 6 : XRD patterns of the AMGS samples raw and calcined at different temperatures. (MO: magnesium oxide, cs: cristobalite cr: corundum, Ao: aluminum oxide, c: μ-cordierite i: indialite, S: Spinel, P: Periclase, q: Quartz, e: Enstatite).

At 1100 °C, the crystallization of the free cristobalite silica (SiO₂) [22] (4.05, 2.85 and 2.49 Å) and the formation of corundum (α-Al₂O₃) (2.08, 2.55 and 1.60 Å) was observed. By increasing the temperature up to 1200 °C, the formation of the μ-cordierite was assured by a partial reaction between the spinel phase and amorphous silica [2, 14, 15]. This is also confirmed by the appearance of new bands at 1085, 935 and 700 cm⁻¹ (Fig. 7) assigned to the μ-cordierite, and the decreasing intensity in the amorphous silica band at 1100 cm⁻¹ [11]. The 1300 °C temperature is characterized by a decrease in the intensity of the diffraction lines of the spinel phase and the formation of α-cordierite phase (8.48, 3.13 and 3.02 Å). This is confirmed by the appearance of the characteristic bands at 1185, 1140, 950 and 770cm⁻¹ [15]. At 1400 °C, the α-cordierite phase becomes predominant, while the minor phase is the spinel.

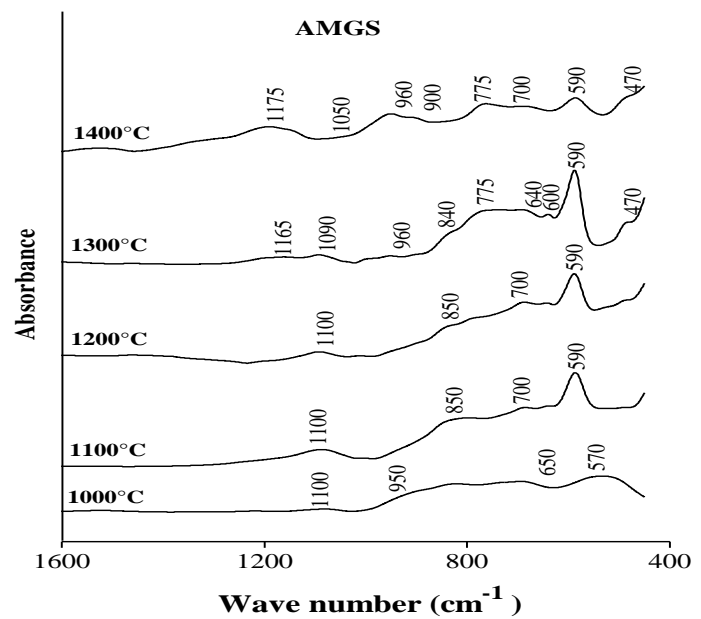


Figure 7 : Infrared spectra of the AMGS sample calcined at different temperature

The results of the mineralogical analysis by X-ray diffraction and IR spectroscopy have shown that the precursor AMGS undergoes several phase transformations during the heat treatment. Thus, at low temperature (1000°C) the formation of spinel and enstatite has been observed. The crystallization of cristobalite, corundum and μ -cordierite takes place at temperatures between 1100 °C and 1200 °C. The formation of α -cordierite is noted at 1300 °C. While at 1400 °C, the phase predominantly obtained is α -cordierite along with the spinel phase in a small proportion.

• **AMAS sample**

The diffraction spectrum of the AMAS sample calcined at 1000 °C shows the formation of enstatite (3.14, 2.87 and 2.49 Å) and spinel (2.43, 1.55, 1.42 Å) (Fig. 8). Additionally, the IR spectra showed the appearance of bands at 560 and 700 cm^{-1} characteristic of the phases spinel [8] (Fig. 9). The rise in temperature up to 1100 °C leads to the crystallization of corundum (2.08, 2.55, 1.60 Å). At 1200 °C, the partial reaction between the spinel and silica leads to the formation of μ -cordierite (1085, 935.700 cm^{-1}) (Fig. 9) [11, 15]. Also at this temperature there is an increase in the intensity of the diffraction lines of the spinel phase and a decrease in that of enstatite (3.15, 3.17, 2.78 Å) and corundum (2.54, 2.082 and 2.54 Å).

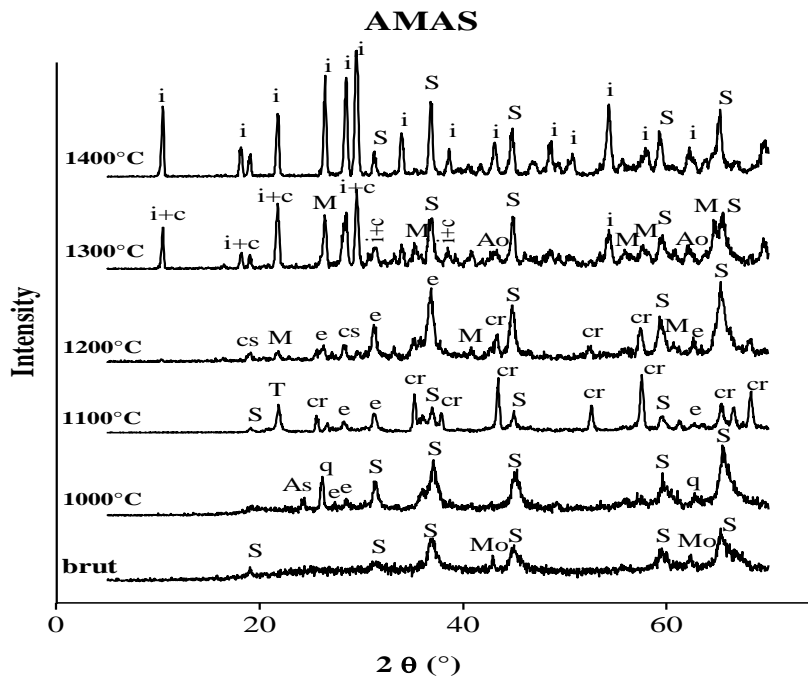


Figure 8: XRD patterns of the AMAS samples raw and calcined at various temperatures. (As: aluminum silicate, MI: magnesium aluminum oxide, As: aluminum silicate, M: mullite, cr: corundum, Ao: aluminum oxide, c: μ -cordierite i: indialite, S: Spinel, q: Quartz, E: Enstatite).

At 1300 °C, the formation of α -cordierite (8.29, 3, 3.3 Å) has been observed. This result is confirmed by the appearance of IR bands at 1185, 1140, 950, 770 cm^{-1} attributed to this phase. At 1400 °C, the α -cordierite constitutes the dominant phase accompanied by a small amount of the spinel phase. Thus, the results of the X-ray diffraction and infrared spectroscopy show that at low temperature there is formation of corundum, enstatite and spinel, while at 1200 °C the crystallization of μ -cordierite had been observed. Furthermore, at 1300 °C, the formation of α -cordierite and total disappearance of enstatite and corundum was noted. And finally, at 1400 °C, the main phase is α -cordierite with some traces of spinel.

Therefore, from the X-ray diffraction and IR spectroscopy studies it could be easy to conclude that the all three precursors AMES, AMAS and AMGS undergoes succession of phase transformations with temperature.

At low temperatures, we observed the crystallization of many crystal phases type spinel, enstatite and corundum for the precursors having as source of silicon, silica gel and silicic acid. Thus, we observed the crystallization of spinel and mullite for the precursor that has as silicon source tetraethylorthosilicate. The rise in temperature leads to the formation of corundum and cristobalite for this latter.

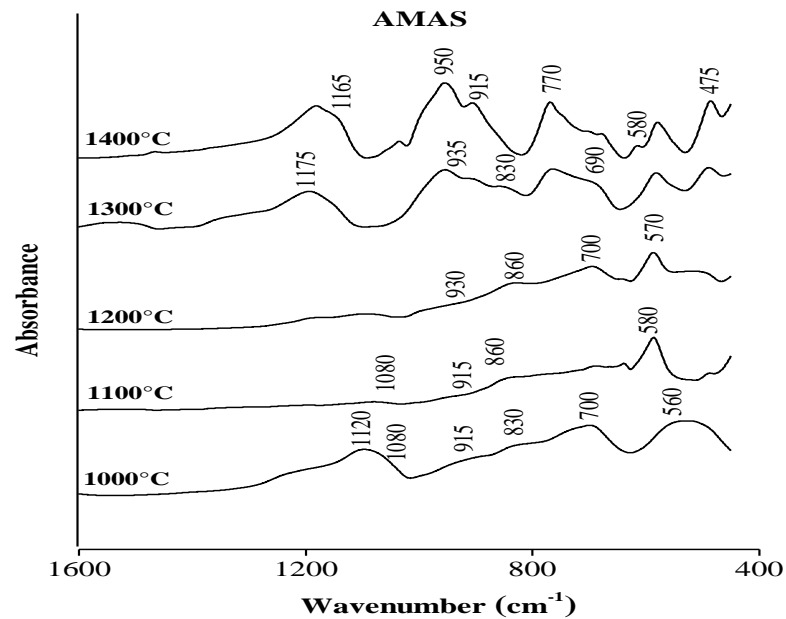


Figure 9: Infrared spectra of the AMAS sample calcined at different temperature.

The three precursors exhibited the same behavior after calcination at 1300 °C, where was noted the formation of the μ -cordierite, and at 1400 °C, where was obtained the α -cordierite as major phase accompanied by the spinel phase as a secondary phase.

The quantity of cordierite phase observed is higher for the precursors having as source of silicon the silicic acid than for the precursors coming from silica gel and tetraethylorthosilicate.

3.2.2. Dilatometric Analysis:

The variations of the linear shrinkage of the studied precursors are represented in Fig. 10. After cooling, there is a difference in linear shrinkage between the various precursors. The linear shrinkage is about 4, 6 and 7% for the samples AMGS, AMES and AMAS respectively. These results reveal that the dilatometric behavior is governed by the phase transformations taking place during the thermal treatment [26].

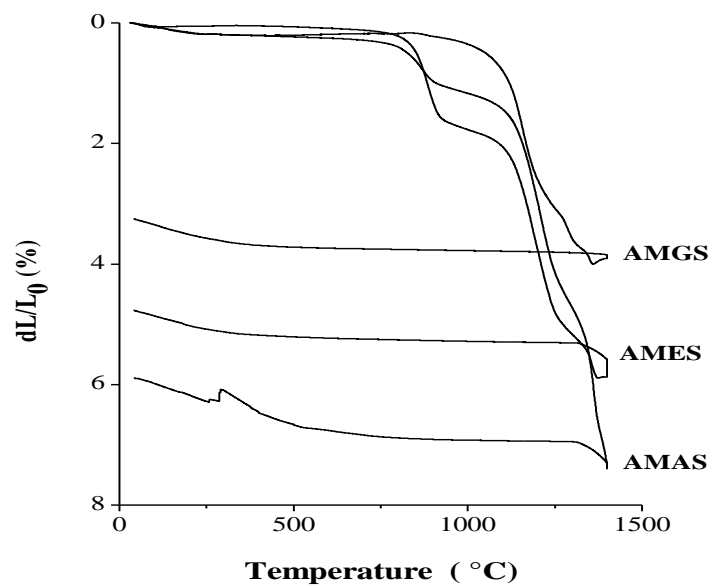


Figure 10: Dilatométric Analysis of samples AMES, AMAS and AMGS at raw state.

Interestingly, the sintering begins at the same temperature for all the three samples but with different rates. The sintering rate is higher for AMES and AMAS. The comparison of the dilatometric behavior of the three precursors allows us to conclude the following points:

- From room temperature to 800 °C: there is a low shrinkage because the samples were pre-calcined and no transformation has been achieved.
- In the range of 800 – 1000 °C many chemical reactions take place leading to the formation of different crystalline phases from a sample to another. For example, mullite, spinel and amorphous silica phases for AMES; enstatite, spinel and magnesium oxide phases for AMGS and finally enstatite and spinel phase for AMAS as a result the shrinkage is different from a sample to another in this range temperature.
- Beyond 1100 °C, the crystallization of the cordierite was noted and the appearance of the liquid phase leading to the rapid and significant shrinkage. The variation of the shrinkage rate from a sample to another is due to the different crystalline phases formed which cause a variation of the chemical composition and the viscosity of the liquid phase in charge of sintering in liquid phase [25, 26].

It is important to note that for all these precursors, the densification is achieved by liquid phase and viscous flow of the amorphous silica. These results confirm that the dilatometric behavior of various precursors is influenced by the phase transformations during heat treatment. Furthermore, the shrinkage ratio is influenced in turn by the silicon source.

3.2.3. Morphological analysis:

Observations by scanning electron microscopy (SEM) were performed on precursors from different sources of silicon calcined at 1400 °C.

The grains observed in different micrographs (Fig. 11, 12 and 13) could only be the cordierite phase, since the three precursors are formed mainly through this phase, as it was revealed by mineralogical analysis. These observations show a certain difference in morphology between the different precursors calcined at 1400 °C, mainly with regard the grain size.

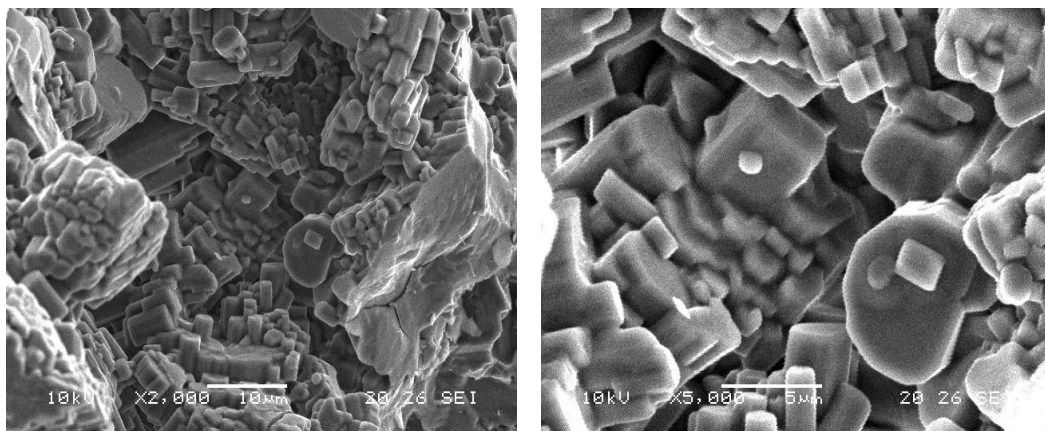


Figure 11: SEM images of the sample AMES calcined at 1400 °C.

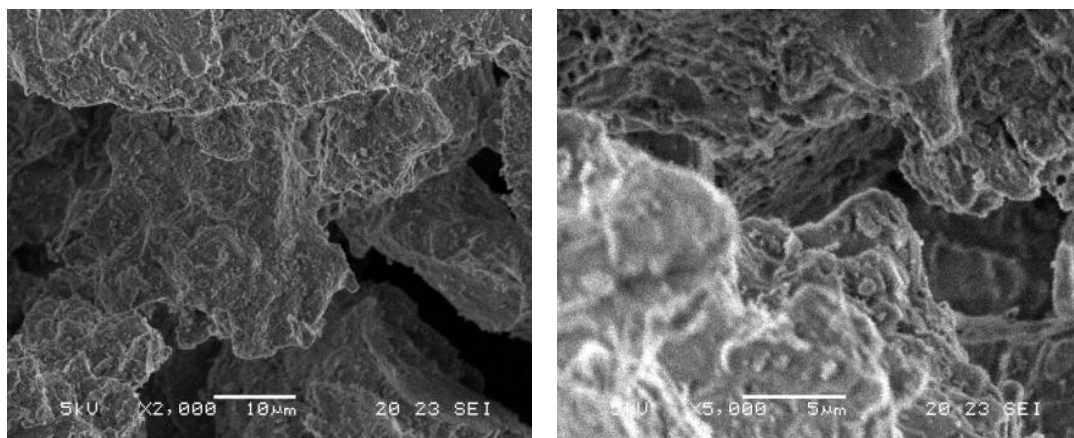


Figure 12: SEM images of the sample AMAS calcined at 1400°C.

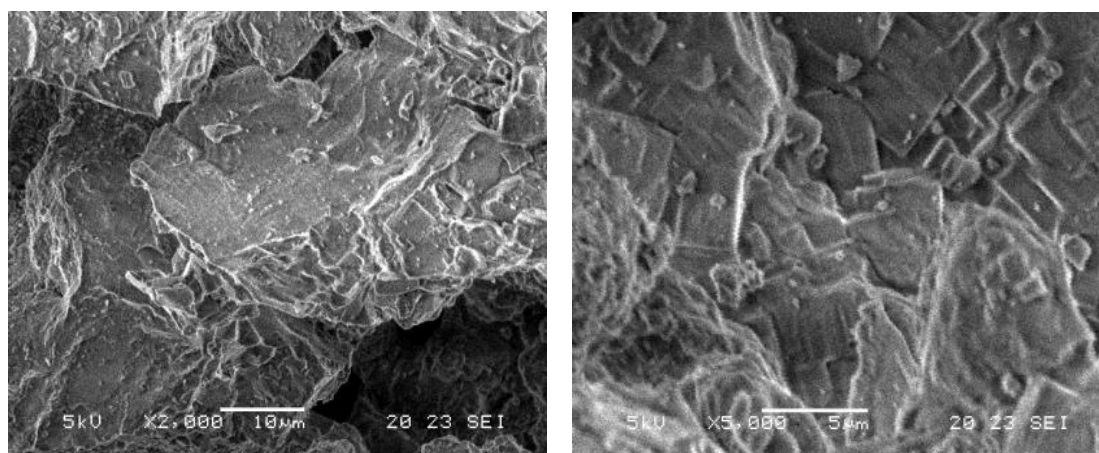


Figure 13: SEM images of the sample AMGS calcined at 1400°C.

The images (Fig. 11, 12 and 13) of precursors with silica gel and silicic acid, show fine grains, nanoparticles, of different shape and size, especially in the case of the sample derived of the silicic acid (1 to 38 µm). The precursor with a source of silicon the tetraethylorthosilicate shows rod-shaped grains with various sizes (with a diameter of 1 to 5 µm). The large grain sizes of cordierite have been observed in the two samples AMAS and AMGS. So it appears that the silicon source affects the morphology of the different samples.

Conclusion

Cordierite precursors were prepared by the coprecipitation method from aluminum chloride, magnesium chlorides and different sources of silicon (silica gel SiO_2 , tetraethylorthosilicate $\text{Si}(\text{OC}_2\text{H}_5)_4$ and silicic acid $\text{H}_2\text{Si}_2\text{O}_5$). The physicochemical characterization of these precursors by applying various experimental techniques allowed us to follow, on the one hand the evolution of the mineralogical composition depending on the temperature, and on the other hand to determine the effect of the nature of the silicon source on the mechanism of crystallization of cordierite.

The crystallization of μ - cordierite for the three precursors begin at 1200 °C. This phase is formed as a result of the transformation of mullite and spinel in the case of the precursor from tetraethylorthosilicate, while the two other precursors having silica gel and silicic acid as the source of silicon, it occurred by reaction of spinel, corundum and enstatite . Beyond 1300 °C, the μ - cordierite reacts with the spinel to form the α -cordierite. However an amount of spinel still exists at 1400 °C, it seems more important in the case of tetraethylorthosilicate. Cordierite grains seem to have a rod-shaped form for the precursor from tetraethylorthosilicate, and an agglomerate of fine grain size for the two other precursors. The variation of the used silicon source leads to the formation of different crystalline phases and consequently to different physicochemical properties

From the foregoing, it follows that the precursor prepared from the silica gel leads after treatment at 1400 °C, to the formation of cordierite of high purity, fine size and low cost.

References

1. Janković-Častvan I., Lazarević S., Jordović B., Petrović R., Tanasković D., Janačković Dj., *J. Eur. Ceram. Soc.* 27 (2007) 3659.
2. Gonzalez-Velasco J.R., Ferret R., Lopez-Fonseca R., Guetierrez-Ortiz M.A., *Powder Technol.* 153 (2005) 34.
3. Banjuraizah J., Mohamad H., Arifin Ahmad Z., *J. Alloys Compd.* 509 (2011) 7645.
4. Banjuraizah J., Mohamad H., Arifin Ahmad Z., *J. Alloys Compd.* 494 (2010) 256.
5. Fuji M., Shiroki Y., Menchavez R.L., Takegami H., Takahashi M., Suzuki H., Izuhara S., Yokoyama T., *Powder Technol.* 172 (2007) 57.
6. Zhu S., Ding S., Xi H., Li Q., Wang R., *J. Eur. Ceram. Soc.* 32 (2007) 115.
7. Dong Y.C., Liu X.Q., Ma Q., Meng G, *J. Memb. Sci.* 285 (2006) 173.

8. Yamuna A., Johnson R., Mahajan Y.R., Lalithambika M., *J. Eur. Ceram. Soc.* 24 (2004) 65.
9. Taruta S., Hayashi T., Kitajima K., *J. Eur. Ceram. Soc.* 24 (2004) 3149.
10. Goren R., Ozgur C., Gocmez H., *J. Eur. Ceram. Soc.* 32 (2006) 407.
11. Goren R., Ozgur C., Gocmez H., *J. Eur. Ceram. Soc.* 32 (2006) 53.
12. Aklouche N., Achour S., Tabet N., *Mater. Res. Bull.* 43 (2008) 1297.
13. Benito J.M., Turrillas X., Cuello G.J., De Aza A.H., De Aza S., Rodrogez M.A., *J. Eur. Ceram. Soc.* 32 (2012) 371.
14. Menchi A.M., Scian A.N., *Mater. Lett.* 59 (2005) 2664.
15. Naskar M.K., Chatterjee M., *J. Eur. Ceram. Soc.* 24 (2004) 3499.
16. González-Velasco J.R., Gutiérrez-Ortiz M.A., Ferret R., Aranzabal A., Botas J. A., *J. Mater. Sci.* 34 (1999) 1999.
17. Ozel E., Kurama S., *J. Mater. Process Technol.* 198 (2008) 68.
18. He Y., Cheng W., Cai H., *J. Hazard Mater.* B120 (2005) 265.
19. Tulyaganov D.U., Tukhtaev M.E., Escalante J.I., Ribeiro M.J., Labrincha J.A., *J. Eur. Ceram. Soc.* 22 (2002) 1775.
20. Shao H., Liang K., Zhou F., Wang G., Peng F., *J. Non Cryst. Solids* 337 (2004) 157.
21. Ghitulica C., Andronescu E., Nicola O., Dicea A., Birsan M., *J. Eur. Ceram.* 27 (2007) 711.
22. Saadi L., Moussa R., Samedi A., *Sil. Ind.* vol. 63 1-2 (1998) 13.
23. Saadi L., Moussa R., Samedi A., Mosset A., *J. Eur. Ceram. Soc.* 19 (1999) 517.
24. Bejjajoui R., Benhammou A., Nibou L., Tanouti B., Bonnet J. P., Yaacoubi A., Ammar A., *Appl. Clay Sci.* 49 (2010) 336.
25. Saadi L., Moussa R., Samedi A., Mosset A., *Ann. Chim. Sci. Mat.*, 25 (2001) 307.
26. Zhou J., Dong Y., Hampshire S., Meng G., *Appl. Clay Sci.* 52 (2011) 328.

(2016) ; <http://www.jmaterenvirosci.com>